Asymptotic relations between time-lag and higher moments of transient nucleation flux

Vitaly A. Shneidman[a)]
Department of Physics, New Jersey Institute of Technology, Newark, New Jersey 07102

Exact relations between T_k, the kth temporal moments of the nucleation flux, and the derivative of its Laplace transform (LT) are established and applied to available asymptotic expressions for the LT, generalizing earlier results by Shneidman and Weinberg [J. Chem. Phys. **95**, 9148 (1991); **97**, 3629 (1992)] on the time-lag T_0. For any $k \geqslant 2$ the moments T_k are expressed through simple algebraic combinations of T_0 and T_1. The two lower moments can thus be used to parametrize the time-dependent flux, with parametrization being substantially different from earlier, nonasymptotic approximations. The leading asymptotic dependences are expected to be applicable to both discrete and continuous versions of the nucleation equation, and to arbitrary sizes in the growth region. Higher-order corrections at the critical size are also obtained. © *2003 American Institute of Physics.* [DOI: 10.1063/1.1627327]

The effects of transient nucleation are important experimentally in systems with long internal relaxation times, as in crystallization of glass-forming melts[1,2] or amorphous silicon,[3] or in systems which can be controlled by a very rapid change of external parameters, as in condensation of electron–hole liquid.[4] Compared to more conventional, steady-state description of nucleation, transient effects are much more sensitive to the detail of kinetics in a specific system. Understanding of such effects and improvement of mathematical methods of their description will potentially enhance control over microstructural properties of new materials.

In theoretical work on transient nucleation in classical-type models[5,6] one can indicate three major directions. The first is related to direct numerical solution of the nucleation master equation with parameters appropriate for the aforementioned experiments.[3,7,8] The advantage of such approaches is their potential straightforward generalization to more realistic (and more complex) experimental schedules.[9] The second direction is based on the possibility to obtain *exact* values of the temporal moments of the transient flux[10–15] (which is a big help; otherwise the time-dependent nucleation master equation cannot be solved exactly). The third direction is based on the asymptotic solution of the nucleation equation in the limit of a high nucleation barrier.[16,17] The transient shape is given by an elementary function—see the following—which is insensitive to the particular nucleation model employed. Model dependence is contained in the "incubation time" defined in terms of a "deterministic growth rate," approximately, the difference of the gain and loss coefficients in the master equation. This helps one understand the relation between various nucleation models and strengthens connection with experiments where growth rates can be measured. Ideally, all three directions should be cross-tested, leading to a comprehensive picture of

transient nucleation. However, although several comparisons between numerical and asymptotic[3,8,16,18–20] or between asymptotic and exact results[14,15] are available, in practice such comparisons are often complicated by a variety of models and parameters discussed. Therefore, outside of the aforementioned publications, the status of the asymptotic solution (especially in connection with discrete nucleation models of Becker–Döring or Turnbull–Fisher[5,6]) or its relations to the exact expressions remain mostly unknown.[13]

The common point for all three directions could be zeroth moment of the flux, the so-called time-lag T_0 (defined in the following) which, on the one hand, can be determined exactly and, on the other, differs by just a constant from the incubation time in the asymptotic solution.[17] Convergence of exact and asymptotic expressions for T_0 had been established for both continuous[14] and discrete[15] nucleation models. In addition, experimentally the time-lag is the primary feature of transient nucleation, and as a rule is reported in numerical studies.

The exact solubility is also a distinct feature of higher temporal moments—see, e.g., Ref. 13 and references therein. At the same time, except for T_0,[14,15] the asymptotic structure of the available complicated exact expressions is not known (for which reason, such expressions are sometimes called *formally exact*), and it is usually not possible to predict their behavior in various domains of parameters, or when switching to another nucleation model. The major goal of this study will thus be to establish an efficient way of generating higher moments using as a starting point the asymptotic transient solution and the time-lag, T_0. In a general form, relations between moments are insensitive either to the nucleation model selected or to one of the primary controlling parameters, the size n at which the moments are evaluated. The more accurate (also more model- and parameter-specific) exact expressions can be potentially used to verify the more robust asymptotic dependences, either confirming the entire approach, or establishing its limitations, in any case narrow-

---

[a)]Electronic mail: vitaly@oak.njit.edu

ing the existing gap between exact and asymptotic studies.

The kth temporal moment is defined as

$$T_k(n) = \int_0^\infty t^k [1 - j(n,t)/j_s] dt \tag{1}$$

with $j(n,t)$ being the transient flux at a given size n, and j_s being its n-independent, steady-state value (in what follows the n dependence will not be indicated, unless confusion can occur). As mentioned, exact relations can be obtained for T_k, although for $k \geq 1$ they are expressed in terms of slowly converging repeated sums which are rather hard to evaluate asymptotically.

An alternative approach is to avoid the exact expressions for T_k, but use the asymptotic solution for $j(n,t)$. The reader is referred to the original paper[16] for technical detail of the derivations, but briefly, the major steps involved can be described as follows. The large parameter of the problem is the dimensionless nucleation barrier W_*/T (Boltzmann constant is taken as one) and the general method of solution is known as matched asymptotic expansions. The domain of sizes n is divided in three regions, the near-critical region characterized by a small width $\Delta \sim n_*/\sqrt{W_*/T}$, the subcritical region $n_* - n \gg \Delta$, and the growth region $n - n_* \gg \Delta$. Under rather relaxed assumptions about the smoothness of the coefficients of the master equation, solutions can be constructed in each of the aforementioned regions, and those solutions can be matched asymptotically, giving the distribution and flux for arbitrary n in the growth region, which is of the main experimental interest.[17] An important intermediate step is switching to the Laplace transform (LT). This simplifies applications of the asymptotic method but also establishes strong similarities of transient nucleation with other nucleation problems. For example, the LT equation is similar to the equation which appears for nucleation with a time-dependent barrier,[16] and can be solved using the same approach. Or, the solution for the LT can be directly applied to nucleation of particles with finite lifetimes (in the presence of an aerosol),[21] without repeating the elaborate intermediate steps of the matched asymptotic analysis. Connection between the LT of the transient flux and the time-lag was established in Ref. 22, and in the following it will be shown that higher moments can be efficiently generated once the LT is known.

The transient solution in the growth region is given by[16,17] $j(n,t)/j_s \equiv \phi$ with

$$\phi(x) = \exp\{-\exp(-x)\}, \quad x = [t - t_i(n)]/\tau \tag{2}$$

and is illustrated in Fig. 1 for different sizes n. Here t_i is the "incubation time" with size-dependence determined by a selected nucleation model, while τ is a constant "relaxation time" defined as $\tau^{-1} = d\nu(n)/dn$ at $n = n_*$, with $\nu(n)$ being the deterministic growth rate. Explicit expressions for t_i (Ref. 17) will not be required, although it could be useful to indicate that t_i is logarithmically large compared to τ when the barrier is large, and that t_i further increases with n into the growth region (an elementary expression for t_i in the Zeldovich–Frenkel model is used in Fig. 1, and will be presented later in the paper). Note that at $t = 0$ Eq. (2) has an asymptotic, rather than an exact zero, although as long as t_i
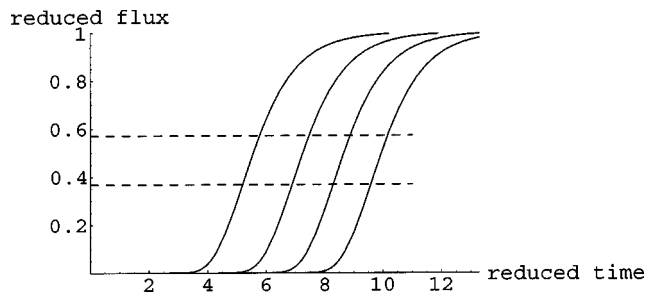

FIG. 1. Typical transient curves $j(n,t)/j_s$ as a function of reduced time t/τ. For each of the curves (from left to right) the dimensionless "radius" $r = (n/n_*)^{1/3}$ is taken, respectively, as $r = 2$, 3, 4, and 5, and in all cases the dimensionless barrier W_*/T is 30. The points of intersection with the lower line, $j(n,t)/j_s = 1/e \approx 0.37$ determine the reduced incubation time t_i/τ, while intersections with the upper line, $\exp[-\exp(-\gamma)] \approx 0.57$ coincide with the reduced time-lag, T_0/τ. Shifting each of the curves by a corresponding incubation time would bring them to single curve given by Eq. (2).

is much larger than τ, the two types of zeroes are impossible to distinguish due to the rapid decay of $\phi(x)$ at negative x [e.g., for the curves in Fig. 1 the values of $j(n,0)/j_s$ range from 10^{-78} to less than 10^{-6000}]. An interpolation which adjusts Eq. (2) to an exact zero at $t = 0$ has been constructed in Ref. 23, but the more complex dependence does not modify the time-lag (and, most likely, will not modify the higher moments), and will not be used in the present study.

Experimentally, one usually measures the number of larger-than-n nuclei, $\rho(t) = \int_0^t j(n,t') dt' \simeq \tau j_s E_1(e^{-x})$,[17] with E_1 being the first exponential integral.[24] The time-lag is then obtained from the large-time asymptote of $\rho(t) \simeq j_s(t - T_0)$ for large t. One has

$$T_0 \simeq \tau \int_{-\infty}^\infty (x + t_i/\tau) \frac{d\phi}{dx} dx \tag{3}$$

with $d\phi/dx = \exp\{-x - \exp(-x)\}$. This evaluates to $T_0 = t_i + \gamma\tau$[17] with $\gamma = 0.5772...$ being the Euler constant. Note that integration in x must be extended to $-\infty$ within the accuracy of the asymptotic treatment. In principle, replacing the factor $(x + t_i/\tau)$ in Eq. (3) by $\tau^k (x + t_i/\tau)^{k+1}/(k+1)$ would give a general asymptotic expressions for the higher moments. For actual calculations, however, it is more straightforward to use the LT from which Eq. (2) was derived.[16]

Near the critical size, n_*, the LT of the flux is expressed in terms of a special function, the repeated error integral. However, extending the asymptote of LT into the growth region (very similarly to what was done in Ref. 16 for the distribution function), and matching that asymptote with the growth asymptote, leads to an elementary expression for the LT at any size $n > n_*$. Using the aforementioned relation between t_i and T_0, one has

$$J(n,p) = j_s \frac{1}{p} e^{p\tau\gamma} \Gamma[p\tau + 1] \exp[-pT_0], \tag{4}$$

where p is the Laplace index and Γ is the gamma function.

The relation between T_k and the LT follows from the definition (1),

$$T_k = (-1)^k \lim_{p \to 0} \left(\frac{\partial}{\partial p}\right)^k \left(\frac{1}{p} - \frac{J(p)}{j_s}\right). \tag{5}$$

TABLE I. Dimensionless truncated moments evaluated from Eq. (A2). The full moments T_k can be reconstructed using Eq. (A3). The value of x_4 evaluates to 12.8865, and for larger k only numerical or asymptotic values are shown.

k	0	1	2	3	4	5	6	7	$k \to \infty$
x_k	0	$\dfrac{\pi^2}{12}$	$\dfrac{2}{3}\zeta(3)$	$\dfrac{3\pi^4}{80}$	$\dfrac{2}{3}\pi^2\zeta(3) + \dfrac{24}{5}\zeta(5)$	67.8122	402.162	2828.83	$k!e^{-\gamma}$

equation (5) is exact, and generalizes the one obtained for $k=0$ in Ref. 22. In other words, temporal moments are linked to coefficients of the Laurent series expansion of the LT,

$$\frac{J(p)}{j_s} = \frac{1}{p} - T_0 + T_1 p + \cdots + \frac{(-1)^{k+1}}{k!}T_k p^k + \cdots. \qquad (6)$$

If one further uses the asymptotic Eq. (4) for the LT, one obtains explicitly the higher moments. The derivative of $\Gamma(p\tau+1)$ at $p=0$ in Eq. (5) can be expressed through the Riemann zeta-function, $\zeta(m)$,[24] and the latter can be evaluated explicitly (as a power of π) for an even argument. Several first moments are shown in the following:

$$T_1 = T_0^2/2 + \pi^2\tau^2/12,$$

$$T_2 = T_0^3/3 + \pi^2\tau^2 T_0/6 + 2\zeta(3)\tau^3/3, \qquad (7)$$

$$T_3 = T_0^4/4 + \pi^2\tau^2 T_0^2/4 + 2\zeta(3)\tau^3 T_0 + 3\pi^4\tau^4/80,$$

etc. Numerical values are to be used for the zeta-function of an odd argument, one has, e.g., $\zeta(3) = 1.2020569...$ in the above. An efficient method for generating such relations for larger k is to express T_k through "truncated moments" obtained from $p^{-1}e^{p\tau\gamma}\Gamma[p\tau+1]$, the size-independent part of the LT—see Table I and Appendix A. Note the structure of the leading term, $T_k \sim T_0^{k+1}/(k+1)$, and the absence of the next power, τT_0^k (which is due to the absence of the linear term in the small-p expansion of $e^{p\tau\gamma}\Gamma[p\tau+1]$). Since one expects $T_0 \gg \tau$, the leading term provides a rather accurate approximation for the higher moment, and only in expressions which contain a *difference* $T_k - T_0^{k+1}/(k+1)$ (see the following) corrections in Eq. (7) become important.

The value of τ thus corresponds to

$$\tau = \frac{\sqrt{6}}{\pi}\sqrt{2T_1 - T_0^2}, \qquad (8)$$

which means that all higher moments with $k \geq 2$ can be expressed through T_0 and T_1. It is important to emphasize that this prediction is asymptotic, i.e., while k is arbitrary, it is expected to be finite, not competing with the main asymptotic parameter, which is the barrier. [In other words, with the increase of the barrier—and most likely with the increase of size—equations of type (7) can be written for a larger k].

If indeed all moments can be expressed through T_0 and T_1, then the entire transient curve can be parametrized using these two moments. This is consistent with the suggestion by Wu,[13] although the actual shape of the transient curve is rather different.

To facilitate comparison, one can introduce temporarily a dimensionless time $\tilde{t} = t/T_0$, and a dimensionless parameter $q = 2T_1/T_0^2$. One has[13]

$$\phi_{\text{Wu}}(\tilde{t}) = 1 - \frac{1}{2}\text{erfc}\left[\frac{\ln(\tilde{t}\sqrt{q})}{\sqrt{2\ln q}}\right]. \qquad (9)$$

Compare this with expected Eq. (2) with

$$x = \frac{\pi}{\sqrt{6}}\frac{\tilde{t}-1}{\sqrt{q-1}} + \gamma. \qquad (10)$$

The parameter q depends primarily on the nucleation barrier and on the size n where the flux is evaluated, approaching 1 for $n \gg n_*$. (For example, for transient curves shown in Fig. 1 q changes between, approximately, 1.07 and 1.01). Wu performed an empirical analysis of transient curves obtained numerically from the Turnbull–Fisher nucleation model, and suggested to use the "lognormal" shape (9) as the best fit. It was claimed that the double-exponential ("Weibull") fit was substantially less accurate, although the exact parametrization for that fit was not reported, and it is not quite clear whether it was tested only at $n = n_*$, or also in the growth region $n = 2n_*$ and $n = 3n_*$ of Fig. 12.[13] [Here the asymptotic results are expected to be the most accurate, and Eq. (2) should work even with calculated, not fitted t_i and τ]. A crude estimation indicates that Wu's values of q in the growth region, approximately, fall between 1.1 and 1.2. In this domain Eqs. (2), (10), and (9) are remarkably close, and the corresponding curves would practically blend with each other if plotted, e.g., the difference $\phi(x) - \phi_{\text{Wu}}(\tilde{t})$ does not exceed 10^{-2} for any $\tilde{t}$, and for values of q near 1.13 the maximum difference is closer to $2 \times 10^{-3}(!)$. Thus, if numerics of Ref. 13 in the growth region confirm Eq. (9), most likely they also do so for Eqs. (2) and (10). This could mean an important improvement in the status of the matched asymptotic solution, especially in connection with more elaborate, discrete nucleation models. At the same time, Eqs. (9) and (2), (10) are obviously different analytically, and a remaining pertinent issue is to determine which of them is more adequate for the nucleation problem.

The difference between the two transient curves should be detectable in dedicated numerical studies, but this can be a challenging task for a single set of data (and for larger q the asymptotic solution can require higher-order corrections, as illustrated in Appendix B). More likely, one needs to consider the tendencies of such curves when the size n is changed. In terms of the physical time t, the asymptotic expression predicts that all transient curves will have identical shapes in the growth region, each being shifted by a time-

independent constant, as in Fig. 1. On the other hand, the shape of lognormal curves will change with size, albeit modestly. A related feature is the values of the flux at $t = T_0$ (i.e., for $\tilde{t} = 1$). One has here from Eqs. (2) and (10), $\phi = \exp[-\exp(-\gamma)] \approx 0.57$[17] for any size, the upper dashed line in Fig. 1. Equation (9), on the other hand, gives a value of $\phi_{\mathrm{Wu}}(1)$ which depends on q, approaching the above value of 0.57 only for q close to 1.14, and going to the limit of 1/2 for $q \to 1$. (In that limit the lognormal dependence is close to $1 - (1/2)\mathrm{erfc}[(x-\gamma)\sqrt{3}/\pi + \sqrt{(q-1)/8}]$). In practice, the two curves given, respectively, by Eqs. (2), (10) or Eq. (9), can be clearly distinguished for q smaller than 1.02 if both are plotted as functions of x against properly scaled numerical data, or if plotted as functions of the physical time t, as in Fig. 1 (as functions of $\tilde{t}$ the two curves will resemble nearly identical steplike functions). Small q correspond to rather large n, which nevertheless can be achieved numerically as shown by Granasy and James.[8] For small q the function ϕ in Eqs. (2) and (10) decays much faster than ϕ_{Wu} as $x \to -\infty$, and in this context one could note a minor overshoot of the lognormal curve over simulation data for $n = 3n_*$ at small times,[13] which could become a systematic tendency at larger sizes. Again, comparative numerical studies would be required here for a definite conclusion.

For q not too close to 1, the lognormal shape should not be a bad assumption since it has an exact zero at $t = 0$, a useful feature in the nonasymptotic case, and since many functions are often well reconstructed by their two lower moments (although the uniqueness of the approximation remains an issue). On the other hand, an advantage of Eq. (9) is that it follows from a consistent asymptotic analysis and thus is expected to become accurate in the limit of a large barrier and for large n, i.e., for $q \to 1$. More importantly, this equation is accompanied by simple, in some cases elementary asymptotic expressions for the moments T_0 and T_1. For example, in the Zeldovich–Frenkel case used in Fig. 1, one has:[17] $T_0/\tau = \ln(6W_*/k_B T) + r - 2 + \ln(r-1) + \gamma$, with r indicating the dimensionless "radius," and the size-dependence of T_1/τ (and of higher moments) also is described in terms of elementary functions, as follows from Eq. (7).

A few remarks on generality and limitations of the obtained results. The exact Eq. (5) is of general validity, although without an explicit expression for the LT of the flux it remains formal. Equation (7) or Eqs. (2) and (10) are expected to be valid asymptotically (for a high nucleation barrier) in the growth region for classical-type nucleation models[5,6] of discrete (Becker–Döring, Turnbull–Fisher) and continuous (Zeldovich–Frenkel) forms. Specifics of a model enters through explicit size dependence of T_0. The latter can be taken in the simpler, asymptotic form, although the exact form is also an option, especially when comparing with Eq. (9).

Since the LT of the transient flux at the critical size is given by the same Eq. (4) with τ replaced by $\tau/2$[22] (and with a different t_i^*), formally, asymptotic results should be also valid at $n = n_*$ with such modification of τ. However, the expected accuracy at n_* is lower since here higher-order corrections to the LT are inversely proportional to the *square*

root of the barrier,[16] in practice not a very large number (see Appendix B).

Finally, the growth-region results are also valid if the moments are introduced for the distribution rather than for the flux in Eq. (1).[13] Indeed, in that region one has $f_s(n) \simeq j_s/\nu(n)$ and $f(n,t) \simeq j(n,t)/\nu(n)$ for the steady-state and transient distributions, respectively, which makes the temporal moments for the distributions asymptotically equivalent to those defined for the fluxes.

Strictly speaking, in order to estimate the accuracy of the obtained formulas one requires further terms in the asymptotic expansions. This is a rather elaborate task, which is also model-specific and will require an additional study. Preliminary analysis indicates that higher-order corrections to the LT in Eq. (4) are proportional to $(W_*/T)^{-1}$ multiplied by a model-dependent decaying function of size. With a nucleation barrier of $20–40T$ such corrections typically amount to a few percent at twice the critical radius, and are smaller at larger r. Within an "experimental level of accuracy" this can be undetectable. Nevertheless, those corrections are worth taking notice of, since they potentially modify the structure of Eq. (7), adding terms with the missing second largest power T_0^k, even if with a small coefficient. This effect is also seen (and is much stronger, of the order of $1/\sqrt{W_*/T}$) at the critical size, which can be examined in more detail since higher-order corrections to the LT are available[15]—see the Appendix B.

In summary, general asymptotic relations between higher moments of the transient nucleation flux have been obtained. Since such moments, at least in principle, can be evaluated exactly, verification of the above-mentioned relations would strengthen the links between the exact and the asymptotic treatments with mutual benefits. Alternatively, verification could be possible from numerical solutions of the nucleation equations with the moments evaluated via direct integration, as in Eq. (1). Specifically, it is expected that for a sufficiently high barrier and for any size n in the growth region the following can be verified: (a) the difference $T_1 - T_0^2/2$ should remain constant, despite the fact that both T_1 and T_0 strongly depend on n, (b) the second two relations of Eq. (7) [with τ evaluated from Eq. (8)] should hold, with accuracy improving with increasing barrier; similar relations should hold for higher T_k although, generally, larger k will require a higher barrier (or larger size) in order for the expressions to become accurate. A more stringent test could use the available asymptotic dependences for T_0 (which are sensitive to the nucleation model selected) and assess the accuracy of the predicted absolute values of higher moments, rather than the relations between them.

APPENDIX A: THE TRUNCATED MOMENTS

One can introduce the "truncated moments," $\tilde{T}_k$, which are centered around T_0. Formally, they can be defined by replacing t^k in Eq. (1) with $(t - T_0)^k$. Compared to the full moments T_k, the truncated $\tilde{T}_k$ are expected to be indepen-

dent of size n (provided n is located in the growth region), and when reduced by τ, asymptotically should give a fixed number x_k, the same for any nucleation model of classical type.[5,6]

Shifting time by T_0 is equivalent to multiplying the LT by $\exp(pT_0)$. This indeed eliminates the size dependence from Eq. (4), and further reduction of the time by τ makes the remaining part of the LT dimensionless,

$$\tilde{J}(s) = s^{-1} e^{s\gamma} \Gamma[s+1] \qquad (A1)$$

with $s = p\tau$. One has

$$x_k = \frac{(-1)^{k+1}}{k+1} \lim_{s\to 0} \left(\frac{\partial}{\partial s}\right)^{k+1} s\tilde{J}(s) \qquad (A2)$$

with the values of x_k given in Table I. Symbolic computations can be helpful for $k \gtrsim 3$, but the large-k approximation can provide sufficient accuracy starting already from $k=6$.

The full moments T_k can be reconstructed using the following relations:

$$T_k = \frac{T_0^{k+1}}{k+1} + \frac{\tau^{k+1}}{k+1} \sum_{m=1}^{k} (m+1) C_{k+1}^{m+1} x_m \left(\frac{T_0}{\tau}\right)^{k-m}, \qquad (A3)$$

where C_n^k are the binomial coefficients. This coincides with Eq. (7) for $k=1$, 2, and 3. In principle, Eq. (A3) can be applied to any k, but the asymptotic nature of the LT from which the number x_k are derived should be kept in mind. Note that x_k rapidly increase with k. Comparing the first and the last terms in Eq. (A3) for $T_0 \gg \tau$, and using the Stirling formula for $k!$, one has the condition $k \sim eT_0/\tau$ when these terms become of the same order. For such and larger k caution must be exercised when using the above expressions, although the above-given limitations are rather relaxed, exceeding 10, for example, for any of the curves in Fig. 1. Evaluation of the terms resulting from higher-order corrections to the LT would be required for a more accurate estimation of the domain of validity.

APPENDIX B: HIGHER-ORDER CORRECTIONS AT THE CRITICAL SIZE

The values appropriate for the critical size will be indicated by an asterisk (*). Introducing $\tilde{\varepsilon} = (3W_*/T)^{-1/2}$ and using Eqs. (4.8)–(10) of Ref. 15, one obtains after some transformations a correction to the LT at $n=n_*$,

$$\delta J^*(p)/j_s = -\frac{4}{3} \tilde{\varepsilon} \tau \exp[-pt_i^*] \Gamma\left[\frac{3+p\tau}{2}\right]. \qquad (B1)$$

Here t_i^* is the incubation time at n_* which contains a large "universal" part $\tau \ln(1/\tilde{\varepsilon})$ and small model-specific corrections. (In particular, t_i^* contains the "discreteness corrections" which distinguish the Becker–Döring or Turnbull–Fisher and the Zeldovich–Frenkel nucleation models.[15] Note, however, that although such corrections can be comparable or even larger than terms which are higher order in $\tilde{\varepsilon}$, changes in the incubation time alone do not modify either the relations between moments or the shape of the transient curve).

When Eq. (B1) is substituted into Eq. (5), the correction to the time-lag $T_0^* = t_i^* + \gamma\tau/2$ is given by $\delta T_0^* = 2\sqrt{\pi}\tilde{\varepsilon}\tau/3$, which is consistent with Ref. 15. Corrections to higher moments also follow:

$$\delta T_1^* \simeq \frac{2\sqrt{\pi}}{3} \tilde{\varepsilon}[\tau T_0^* - \tau^2(1-\ln 2)],$$

$$\delta T_2^* \simeq \frac{\sqrt{\pi}}{12} \tilde{\varepsilon}\tau[8(T_0^*)^2 - 16T_0^*\tau(1-\ln 2) + \tau^2(\pi^2 - 8\ln 2(2-\ln 2))], \qquad (B2)$$

etc. The leading terms in the above should be compared, respectively, with $\pi^2\tau^2/48$, $0.8\tau^3$, etc., the smallest terms in Eq. (7) with τ replaced by $\tau/2$. Estimating T_0^* as $\tau \ln(1/\tilde{\varepsilon})$, one concludes that for a typical barrier of $30T$ with $\tilde{\varepsilon} \approx 0.1$, the higher order corrections to T_1^* and T_2^* will have contributions which are comparable with the smallest leading terms, and thus cannot be ignored. In particular, δT_1^* will affect the difference $T_1^* - (T_0^*)^2/2$, and the transient curve.

In order to obtain the correction to the transient curve one needs to invert asymptotically the correction to the LT given by Eq. (B1). This can be done via summation over residues of the gamma function located in the finite part of the complex p plane, as in Ref. 16. One obtains

$$\delta\phi(x^*) \simeq -\frac{8}{3}\tilde{\varepsilon}e^{-3x^*/2}\phi(x^*) \qquad (B3)$$

with $x^* = (t - t_i^*)/(\tau/2)$.

[1] P. James, Phys. Chem. Glasses **15**, 95 (1974).
[2] J. Deubener, J. Non-Cryst. Solids **274**, 195 (2000).
[3] C. Spinella, S. Lombardo, and F. Priolo, J. Appl. Phys. **84**, 5383 (1998).
[4] R. M. Westerwelt, Phys. Status Solidi B **74**, 727 (1976); **76**, 31 (1976); I. M. Fishman, Usp. Fiz. Nauk **155**, 329 (1987).
[5] M. Volmer and A. Weber, Z. Phys. Chem. **119**, 227 (1926); L. Farkas, *ibid.* **125**, 236 (1927); R. Becker and W. Döring, Ann. Phys. (Leipzig) **24**, 719 (1935); Ya. B. Zeldovich, Acta Physicochim. URSS **18**, 1 (1943); J. Frenkel, *Kinetic Theory of Liquids* (Oxford University Press, Oxford, 1946).
[6] D. Turnbull and J. C. Fisher, J. Chem. Phys. **17**, 71 (1949).
[7] K. F. Kelton, A. L. Greer, and C. V. Thompson, J. Chem. Phys. **79**, 6261 (1983).
[8] L. Granasy and P. James, J. Chem. Phys. **113**, 9810 (2000).
[9] K. F. Kelton and A. L. Greer, Phys. Rev. B **38**, 10089 (1988).
[10] R. Andreas and M. Boudart, J. Chem. Phys. **42**, 2057 (1965); H. L. Frisch and C. Carlier, *ibid.* **54**, 4326 (1971); G. Wilemski, *ibid.* **62**, 3772 (1975).
[11] B. Shizgal and J. C. Barrett, J. Chem. Phys. **91**, 6505 (1989).
[12] D. T. Wu, J. Chem. Phys. **97**, 1922 (1992).
[13] D. T. Wu, in *Solid State Physics: Advances in Research and Applications*, edited by H. Ehrenreich and F. Spaepen (Academic, San Diego, 1996), pp. 37–187.
[14] V. A. Shneidman and M. C. Weinberg, J. Chem. Phys. **97**, 3621 (1992).
[15] V. A. Shneidman and M. C. Weinberg, J. Chem. Phys. **97**, 3629 (1992).
[16] V. A. Shneidman, Sov. Phys. Tech. Phys. **32**, 76 (1987).
[17] V. A. Shneidman, Sov. Phys. Tech. Phys. **33**, 1338 (1988).
[18] I. L. Maksimov, M. Sanada, and K. Nishioka, J. Chem. Phys. **113**, 3323 (2000).
[19] V. A. Shneidman and P. Hänggi, J. Chem. Phys. **101**, 1503 (1994).
[20] K. F. Kelton, Mater. Sci. Eng., B **32**, 145 (1995).
[21] V. A. Shneidman and I. M. Fishman, Chem. Phys. Lett. **173**, 331 (1990).
[22] V. A. Shneidman and M. C. Weinberg, J. Chem. Phys. **95**, 9148 (1991).
[23] V. A. Shneidman, J. Chem. Phys. **115**, 8141 (2001).
[24] M. Abramowitz and I. Stegun, *Handbook of Mathematical Functions* (Dover, New York, 1972).